Strong-coupling series for Abelian lattice gauge models in 3+1 dimensions

C. J. Hamer,[*] J. Oitmaa,[†] and Zheng Weihong[‡]

School of Physics, The University of New South Wales, P.O. Box 1, Kensington, NSW 2033, Australia
(Received 22 July 1993)

Linked cluster methods are used to calculate extended strong-coupling series expansions for the ground-state energy, specific heat, scalar, and axial-vector mass gaps in the Z_N and U(1) Abelian gauge models in 3+1 dimensions. There is evidence of a singularity at physical couplings in the specific heat series, but none in the mass gap series. A comparison with Monte Carlo data in the U(1) case indicates that there is actually a weak first-order transition.

I. INTRODUCTION

Abelian lattice gauge theories in 3+1 dimensions have been a favorite testing ground for numerical techniques, but the details of their critical behavior have proved remarkably elusive. The pure Z_N gauge models were the showcase in which Creutz, Jacobs, and Rebbi [1] first demonstrated the utility of Euclidean Monte Carlo methods. The Euclidean models have also been explored using strong-coupling series expansions [2], as well as other approaches. The models are self-dual [3], and this fact was useful in establishing the phase structure: For $N \leq 4$, the Z_N models display a single first-order phase transition at the self-dual point, while for $N \geq 5$ there are two transitions, at points which are conjugate to each other under the dual transformation, with a massless Coulomb phase in between. This phase structure is analogous to that of the Z_N symmetric spin models in 1+1 dimensions, although the gauge model transitions for $N \geq 5$ have been thought to be second order [2,4], with index $\nu \simeq 1/3$, as opposed to the Kosterlitz-Thouless transition in the spin models. Studies of the Hamiltonian forms of these models [5–7] have broadly agreed with this picture.

In the limit $N \to \infty$ the Z_N gauge model becomes equivalent to the compact U(1) theory, with the self-dual point receding towards $g^2 = 0$. This leaves only two phases for the U(1) theory, a confining phase and the massless Coulomb phase. The nature of the transition between these phases has been a matter of long debate. It was originally thought [1,8] to be a second-order transition, but then Jersak *et al.* [9] observed a small, sharp hysteresis effect in the "mean plaquette value" indicating a weak first-order transition instead. The order of the transition depends on the exact form chosen for the action; but for the simple Wilson action, several further studies have appeared, some favoring a second-order transition [10], others a first-order one [11]. The most recent Monte Carlo calculations [12,13] appear to show

a very weak first-order transition, which only becomes apparent in the specific heat above lattice size $L = 10$. None of the Hamiltonian studies [14–17] have seen any sign of first-order behavior, but they have not reached such large lattice sizes.

In view of this debate, the order of the transition in the Z_N models probably needs to be reevaluated as well.

In the present paper we report some extensions to the strong-coupling series obtained previously [7] for the Hamiltonian models. We have been able to add an extra two terms to the series for the vacuum energy and specific heat, and also to generate new series for the scalar and axial-vector mass gaps, the first since the hand calculations of Kogut, Sinclair, and Susskind [14]. Section II discusses the methods to generate the series, while in Sec. III the series are analyzed. In the case of the U(1) model, a comparison of the series analysis with earlier Monte Carlo data [17] provides fairly clear evidence that the transition is indeed a weak first-order one. Further Monte Carlo data are needed to check whether a similar conclusion applies to the Z_N models also. These arguments are set out in more detail in Sec. IV.

II. METHODS

The Z_N lattice gauge theories (LGT's) in 3+1 dimensions [(3+1)D] can be described by the Hamiltonian

$$H_N = \frac{g^2}{2a} W_N ,$$

$$W_N = \frac{1}{\xi_N} \left[\sum_l E_N(l) - \lambda \sum_p [U_N(p) + U_N^\dagger(p)] \right] ,$$

$$(2.1)$$

where l labels the links between sites, p labels the elementary plaquettes of the lattice, a is the lattice spacing, g is the bare electric charge, the strong-coupling parameter $\lambda = \xi_N/g^4$, and

$$\xi_N = 2 \left(1 - \cos \frac{2\pi}{N} \right) ,$$

$$E_N(l) = 2 \left(1 - \cos \frac{2\pi}{N} L_N(l) \right) ,$$

$$(2.2)$$

$$U_N(p) = U_1 U_2 U_3^\dagger U_4^\dagger .$$

[*]Electronic address: c.hamer@unsw.edu.au
[†]Electronic address: otja@newt.phys.unsw.edu.au
[‡]Electronic address: w.zheng@unsw.edu.au

The U_l ($l = 1, 2, \ldots, 4$) operators are defined on the oriented links of each plaquette p and act as raising operators on the space of eigenstates of the $L_N(l)$:

$$L_N|L\rangle = L|L\rangle , \qquad (2.3)$$

$$U_l|L\rangle = |L'\rangle , \quad \text{where} \quad L' = (L+1)(\text{mod } N) . \qquad (2.4)$$

From the Z_N symmetry it follows that

$$(U_N)^N = I . \qquad (2.5)$$

One of the most important properties of the Z_N model is its self-duality about the point $\lambda = 1$; that is, the Hamiltonian satisfies [14]

$$H_N(\lambda) = \lambda H_N(1/\lambda) + C_N(\lambda) , \qquad (2.6)$$

where the constant $C_N = 6M^3(1-\lambda)/\xi_N$, and M^3 is the volume of the lattice.

In the limit $N \to \infty$, the Z_N model is equivalent to the compact U(1) model, which is described by

$$H = \frac{g^2}{2a}W ,$$

$$W = \sum_l E^2(l) - x \sum_p [U(p) + U^\dagger(p)] , \qquad (2.7)$$

where E_l and $U_{l'}$ satisfy the U(1) algebra

$$[E_l, U_{l'}] = U_l \delta_{l,l'} \qquad (2.8)$$

and this equivalence is established via the relation

$$\lambda/\xi_N \equiv x = 1/g^4 ,$$

$$E_N(l)/\xi_N \to E^2(l) , \qquad (2.9)$$

$$U_N(p) \to U(p) .$$

To calculate the strong-coupling series for the model, we used Nickel's cluster expansion method. The techniques necessary were reviewed by He $et\ al.$ [18], and will not be repeated here. In these calculations, the first term in Eqs. (2.1) and (2.7) is taken as the unperturbed Hamiltonian, diagonal in the basis of eigenvectors of $E(l)$, while the second term in Eqs. (2.1) and (2.7) then acts as a perturbation which raises or lowers E_l one unit on links $1, \ldots, 4$ of the plaquette. In the strong-coupling limit $x \to 0$, the dominant term in the Hamiltonian is the electric field term. The strong-coupling states are therefore eigenstates of $E(l)$, which takes integer eigenvalues on each link l. Series have been calculated for the ground-state energy, and the lowest-lying symmetric and axial-vector excited state eigenvalues m_s, m_A for both the Z_N ($N = 2, 4, 5, 6, 7, 8$) and U(1) models (the
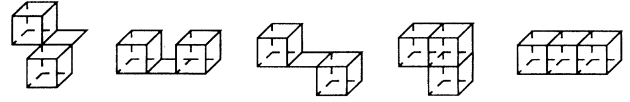
FIG. 2. The last five graphs which contribute to order x^{15} of the ground-state energy.

Z_2 model does not have an axial-vector excited state due to its modulus 2).

To generate the series for the ground-state energy, we need to generate a list of connected plaquette configurations, together with their lattice constants and embedding constants. For (3+1)D Abelian theory, as discussed in Ref. [16], an open topology of cluster size j will contribute to order x^{2j} or higher, but for a closed topology, the situation is a bit more complicated; for example, the cube which is a closed topology of cluster size $j = 6$ contributes at order x^6. To save computer time, we only generate the clusters which contribute to the order considered. Even so, if we treat any pairs of clusters as topologically distinct unless they are degenerate under lattice translations, rotations, or reflections (there are in total 48 such symmetry operations), there is still an enormous number of clusters (61691) contributing to order x^{15}. Actually, many of the graphs give the same contribution to the ground-state energy: For example, the clusters in Fig. 1 have the same contribution; that is, the contribution from each cluster only depends on how many plaquettes are joined together, rather than how they are joined. Considering this, the number of clusters can be dramatically reduced. Altogether, to get the ground-state series up to order x^{15}, we need to generate five different classes of connected plaquette configurations.

(1) All plaquette configurations up to size 7, totaling 58775 clusters; these can be reduced to 824 graphs if we consider the equivalence of some clusters.

(2) The plaquette configurations with one cube and size between 8 and 10, totaling 2817 graphs, which can be reduced to 293 graphs.

(3) The plaquette configurations with a dicube and size between 10 and 12, totaling 86 graphs, which can be reduced to 38 graphs.

(4) The plaquette configurations with two cubes joined by one common edge and size between 12 and 13, totaling eight graphs, which can be reduced to six graphs.

(5) There are still five plaquette configurations shown in Fig. 2 which contribute to order x^{15}, the first three having equal contributions to the ground-state energy.

The second, third, and fourth classes of graphs have been generated starting from a cube, a dicube, and two cubes joined by one common edge, respectively. In total, there are 61691 graphs contributing to the ground-state
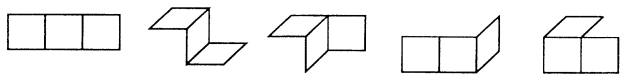

FIG. 1. Examples of graphs which are not degenerate under lattice translations, rotations, or reflections, but have the same contribution to the ground-state energy and symmetric mass gap.
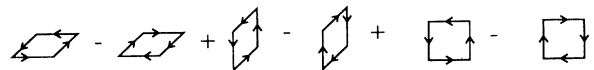

FIG. 3. The single plaquette excitations for the axial-vector excited state in the strong-coupling limit (here the rotationally symmetric representation is used).

FIG. 4. Two plaquette configurations which contribute differently to the axial-vector excited state.

energy at order x^{15}, and the number of graphs can be reduced to 1164 if we consider equivalence between graphs.

In the strong-coupling limit, the symmetric excited states consist of single plaquette excitations on the lattice, symmetric under a parity transformation. To generate the series for the mass gap, we need to generate a list of plaquette configurations, both connected and disconnected, together with their lattice constants and embedding constants. For the calculation of the symmetric excited state eigenvalues m_s, there are in total 6207 graphs, both connected and disconnected, contributing up to order x^{11}. These graphs can be reduced to 325 if we consider the equivalence between graphs.

The calculation of the axial-vector excited state eigenvalue m_A is more complicated. In the strong-coupling limit, if we choose the rotationally symmetric representation, the lowest-lying axial-vector excited states consist of single plaquette excitations on the lattice, antisymmetric under a parity transformation, as shown in Fig. 3. Then for the two plaquette configurations where the plaquettes are joined together vertically, for example, there are two different configurations shown in Fig. 4, which contribute to the axial-vector mass gap differently. The difference arises when the operator U_p is applied to the strong-coupling vacuum for both plaquettes, because the common edge has eigenvalue 2 of $E(l)$ in one graph, and eigenvalue 0 in another graph. Therefore, we cannot treat any pair of clusters as equivalent under all 48 symmetry

operations of rotations and reflections, as in the calculation of the ground-state energy and symmetric mass gap. In order to distinguish the difference in Fig. 4, the number of symmetry operations must be reduced to 12; and so there are 22542 graphs, connected and disconnected, contributing up to order x^{10}. Certainly, some clusters still have equivalent contributions to the axial-vector mass gap, but to be safe, we could not further reduce the number of clusters by any other symmetry.

The series calculation, which was carried out in quadruple precision, occupied several thousand hours of CPU time on an IBM RS6000 workstation; it would need about 10 times more CPU and memory to extend the series one more order. The resulting series for Z_N ($N = 2, 4, 5, 6, 7, 8$) and U(1) LGT's are listed in Table I and Table II. The ground-state energy series for U(1) agrees with that of Irving and Hamer [16] up to order x^6, but disagrees slightly for the x^8 and x^{10} coefficients; the two last coefficients are new. For the Z_N models, the series agree with Irving and Hamer [7] up to order x^{10} for Z_2 and order x^6 for $N > 2$, but disagree at order x^8 and x^{10} for $N > 2$; and again the two last coefficients are new. After so much time has elapsed, it has not been possible to determine exactly why the discrepancy with earlier work has occurred. The mass gap series are the first since the hand calculations of Kogut et al. [14] for the U(1) model: They agree with Kogut et al. up to order x^4, and the terms beyond that are new.

III. SERIES ANALYSIS

A. Z_N models

Figure 5 displays estimates of the vacuum energy per site for the Z_N models, which were obtained using integrated first-order inhomogeneous differential approximants [19] to extrapolate the series listed in Table I. Some

TABLE I. Coefficients of series expansions in x for the vacuum energy density ω_0/M^3, the symmetric mass gap m_s, and the axial-vector mass gap m_A of the Z_N ($N = 2, 4, 6, 8$) and U(1) LGT's in (3+1)D.

Order	Z_2	Z_4	Z_6	Z_8	U(1)
		The vacuum energy density ω_0/M^3			
0	0	0	0	0	0
2	-3	$-3/2$	$-3/2$	$-3/2$	$-3/2$
4	$-9/4$	$-9/32$	$-3/32$	$-4.595999633863\times10^{-2}$	$9/640$
6	$-4117/240$	$-4117/7680$	$-3.643386440912\times10^{-1}$	$-3.469752713639\times10^{-1}$	$-21991741/64512000$
8	$-24649619/288000$	$-6.682006022135\times10^{-1}$	$-6.587903188678\times10^{-2}$	$3.202418092571\times10^{-2}$	$1.431376756392\times10^{-1}$
10	$-7.380641344143\times10^2$	-1.435484920718	$-4.787738324991\times10^{-1}$	$-4.421715941067\times10^{-1}$	$-4.665560506719\times10^{-1}$
12	$-5.883415619655\times10^3$	-2.846201977681	$-8.457724360124\times10^{-2}$	$1.786674368715\times10^{-1}$	$4.717126929228\times10^{-1}$
14	$-5.637946435350\times10^4$	-6.780667242546	-1.064654305862	$-9.972859324203\times10^{-1}$	-1.201323178083
		The symmetric mass gap m_s			
0	4	4	4	4	4
2	-22	$-11/2$	$-157/40$	-3.536330140811	$-37/12$
4	$-2069/6$	$-2069/96$	$-82751917/4032000$	$-2.057477177993\times10^1$	$-3348799/161280$
6	$2031479/720$	$2049943/46080$	5.038614799980×10^1	5.058223002473×10^1	5.078182045892×10^1
8	7.955491557935×10^4	3.182517893282×10^2	3.394631949653×10^2	3.455147220794×10^2	3.528303990612×10^2
10	$-2.150508794062\times10^6$	$-2.100012827466\times10^3$	$-1.915475325940\times10^3$	$-1.862667592725\times10^3$	$-1.799555518774\times10^3$
		The axial-vector mass gap m_A			
0		4	4	4	4
2		$-7/2$	$-129/40$	-3.081145640666	$-35/12$
4		$-231/32$	$-7469591/1344000$	-5.239810675572	$-2364413/483840$
6		$-397867/138240$	4.473779024242	5.606592253594	6.751142877121
8		$-8.384727803297\times10^{-1}$	2.235229851505	$9.889037415424\times10^{-1}$	-1.081729620434
10		$-4.562812798376\times10^1$	$-5.104516905059\times10^1$	$-5.119332933441\times10^1$	$-5.012538641319\times10^1$

TABLE II. Coefficients of series expansions in x for the vacuum energy density ω_0/M^3, the symmetric mass gap m_s, and the axial-vector mass gap m_A of the Z_N ($N = 5, 7$) LGT's in (3+1)D.

| Order	ω_0/M^3	m_s	m_A
		Z_5 model	
0	0	4	4
1	0	0	0
2	$-3/2$	-4.351525249006	-3.386847414460
3	0	$-2.387287570313\times10^{-2}$	$2.387287570313\times10^{-2}$
4	$-1.426310244865\times10^{-1}$	$-2.058210218541\times10^{1}$	-5.927874497759
5	$3.419485166023\times10^{-3}$	$-3.484213628597\times10^{-2}$	$-3.645671021723\times10^{-2}$
6	$-3.934331963395\times10^{-1}$	$5.004730411251\times10^{1}$	3.069297969521
7	$3.760237609476\times10^{-3}$	$-2.179053095073\times10^{-1}$	$-1.791583122540\times10^{-1}$
8	$-1.811834042454\times10^{-1}$	$3.330714730434\times10^{2}$	2.920029116968
9	$1.438302274590\times10^{-2}$	$1.738836382235\times10^{-1}$	$-3.319489250433\times10^{-2}$
10	$-5.796496089532\times10^{-1}$	$-1.971461611702\times10^{3}$	$-5.027356535792\times10^{1}$
11	$1.938677578719\times10^{-2}$	-4.907664507119	
12	$-4.384831114460\times10^{-1}$		
13	$5.546575306543\times10^{-2}$		
14	-1.437239338661		
15	$8.733518692988\times10^{-2}$		
		Z_7 model	
0	0	4	4
1	0	0	0
2	$-3/2$	-3.685320557282	-3.135947163746
3	0	0	0
4	$-6.466376799215\times10^{-2}$	$-2.054264253324\times10^{1}$	-5.360339001763
5	0	$-4.719369191458\times10^{-5}$	$4.719369191458\times10^{-5}$
6	$-3.523798114130\times10^{-1}$	$5.051533066610\times10^{1}$	5.189741144643
7	$5.450491419073\times10^{-6}$	$-4.253424136205\times10^{-5}$	$-5.713208437285\times10^{-5}$
8	$-4.855516843368\times10^{-3}$	$3.431694043354\times10^{2}$	1.533672643527
9	$5.324221070236\times10^{-6}$	$-2.409631884875\times10^{-4}$	$-2.622464938526\times10^{-4}$
10	$-4.497238902725\times10^{-1}$	$-1.883091227284\times10^{3}$	$-5.123144000884\times10^{1}$
11	$2.373674376739\times10^{-5}$	$1.245033658014\times10^{-4}$	
12	$8.193064774641\times10^{-2}$		
13	$1.993705997377\times10^{-5}$		
14	$-9.949284832879\times10^{-1}$		
15	$7.580240399646\times10^{-5}$		
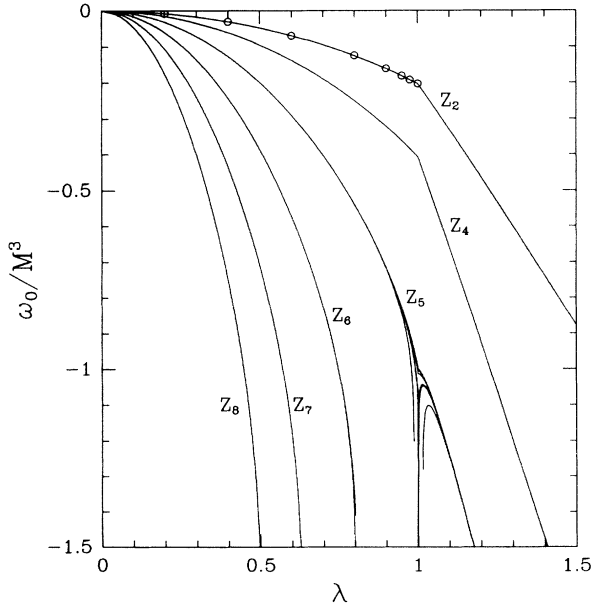
FIG. 5. Graph of the ground-state energy per site ω_0/M^3 against λ for the Z_N ($N = 2,4,5,6,7,8$) LGT in (3+1)D. The self-duality relation about $\lambda = 1$ was used to obtain the results beyond $\lambda = 1$. Also shown are the Monte Carlo results [20] for the Z_2 model. One can distinguish several different approximants for the Z_5 model.
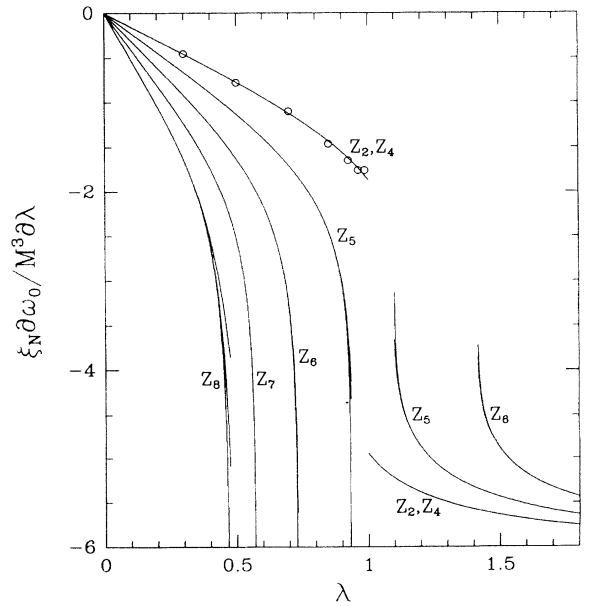

FIG. 6. Graph of the derivative of the ground-state energy per site $\xi_N \partial\omega_0/M^3\partial\lambda$ against λ for the Z_N ($N = 2,4,5,6,7,8$) LGT in (3+1)D. Also shown are the Monte Carlo results [20] for the Z_2 model.

Monte Carlo results for the Z_2 model [20] are shown for comparison — the agreement is very good. The duality relation (2.6) has been used to continue the results beyond the self-dual point, $\lambda = 1$. The results for the Z_2 and Z_4 models show a clear break at $\lambda = 1$, indicating a first-order transition. For $N \geq 6$, the series approximants show divergent behavior, indicating a phase transition well before the self-dual point. For $N = 5$, the divergence occurs very close to $\lambda = 1$, and the situation is not yet clear.

Figure 6 shows the derivative of the vacuum energy with respect to coupling λ. The Z_2 and Z_4 models, which are indistinguishable on this plot, show a large discontinuity at $\lambda = 1$, equivalent to a "latent heat." The discontinuity for $\xi_N \partial \omega_N / \partial \lambda M^3$ is estimated to be 3.08(1) for the Z_2 and Z_4 models, compared to the earlier estimate of 3.19(5) by Irving and Hamer [7]. Hamer and Court [20] appear to have made an erroneous use of duality in estimating this quantity; but their Monte Carlo results at small λ agree well with the series estimates, as seen in Fig. 6. The $N \geq 5$ results diverge before $\lambda = 1$, indicating an earlier transition.

Figure 7 displays the "specific heat"

$$C(\lambda) = -2\lambda^2 \frac{\partial^2}{\partial \lambda^2} \left[\frac{\omega_0(\lambda)}{M^3} \right] , \qquad (3.1)$$

which exhibits a finite cusp at $\lambda = 1$ for the Z_2 and Z_4 models, but appears to diverge at smaller λ for $N \geq 5$. Dlog Padé approximants to the series for $C(\lambda)$ give poles and residues as shown in Table III. For Z_2 and Z_4 the position of the pole is generally well beyond $\lambda = 1$, consistent with the first-order character of the transition. For Z_6 there is a pole at $\lambda^2 = 0.49(3)$, with residue $-0.9(2)$,
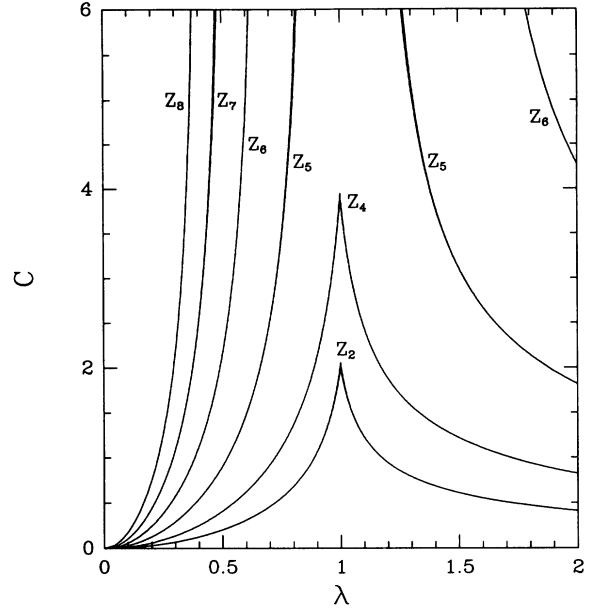

FIG. 7. Graph of the specific heat C against λ for the Z_N ($N = 2, 4, 5, 6, 7, 8$) LGT in (3+1)D.

consistent with a second-order transition at that point with index $\alpha = 0.9(2)$. For Z_8 similarly, the results are consistent with a critical point at $\lambda^2 = 0.19(2)$, with index $\alpha = 0.8(3)$. For Z_5, the transition appears to be at $\lambda = 0.915(10)$, $\alpha = 0.87(4)$, while for Z_7, it is at $\lambda = 0.559(6)$, $\alpha = 1.00(5)$. These values are close to, and overlap in most cases, the value $\alpha = 1$ which would correspond to a first-order transition. The only

TABLE III. The position and residues of the leading poles at physical coupling in Dlog Padé approximants to the specific heat series for the Z_N and U(1) models.

	Order M	$M - 1/M$ Pole (residue)	M/M Pole (residue)	$M + 1/M$ Pole (residue)
Variable: λ^2				
Z_2	2	1.229 (-0.703)	1.204 (-0.656)	1.173 (-0.588)
	3	1.278 (-0.717)[a]		
Z_4	2	1.234 (-0.709)	1.213 (-0.670)	1.184 (-0.604)
	3	1.262 (-0.725)[a]		
Z_6	2	0.513 (-0.981)	0.496 (-0.889)	0.437 (-0.534)
	3	0.518 (-0.997)[a]		
Z_8	2	0.202 (-1.067)	0.193 (-0.945)	0.158 (-0.435)
	3	0.204 (-1.082)[a]		
Variable: x^2				
U(1)	2	0.699 (-1.19)	0.661 (-1.02)	0.472 (-0.28)
	3	0.705 (-1.21)[a]		
Variable: λ				
Z_5	4	0.919 (-0.893)	0.917 (-0.885)	0.905 (-0.817)
	5	0.919 (-0.894)[a]	0.906 (-0.822)	0.905 (-0.818)
	6	0.926 (-0.912)[a]	0.921 (-0.898)[a]	
Z_7	4	0.5623 (-1.033)	0.5623 (-1.033)	0.5515 (-0.924)
	5	0.5623 (-1.033)	0.5515 (-0.924)	0.5515 (-0.924)
	6	0.5648 (-1.048)[a]	0.5648 (-1.048)[a]	

[a]Defective.

critical-point estimate available for comparison is an exact linked-cluster expansion (ELCE) calculation [7] for the Z_6 model, $\lambda_c^2 = 0.44(5)$, obtained from an analysis of the string tension. This is a little less than the estimate obtained above, but agrees with it within errors.

The behavior of the scalar mass gap m_s is illustrated in Fig. 8. For Z_2 and Z_4 the curves are again hardly distinguishable, and a very substantial mass gap, $m_s = 2.1(1)$, remains at $\lambda = 1$. For $N \geq 5$, convergence is lost well before $\lambda = 1$. A Dlog Padé analysis, however, shows no signs of a consistent pole, i.e., a singularity, at small positive λ. The dominant singularities appear to be a complex pair of poles in the λ plane. The series are quite short, however, and the signs of the coefficients alternate in pairs, so that it is difficult to draw any firm conclusions. If the integrated differential approximants to the mass gap are cut off at the critical point deduced from the specific heat series, as in Fig. 8, it certainly appears as if the mass gap remains finite at the critical point, although the convergence of the approximants is not very good by then.

The behavior of the axial-vector mass gaps (Fig. 9) is very similar. The axial-vector mass gaps generally lie a little higher than the scalar gaps; and the convergence of the approximants is if anything rather better. Once again, the mass gaps appear to remain finite at the critical points deduced from the specific heat series.

B. U(1) model

Figure 10 shows estimates of the vacuum energy per site for the U(1) model, obtained in the same way as for the Z_N models. Some Monte Carlo results from Hamer

FIG. 9. Graph of the axial-vector mass gap m_A against λ for the Z_N ($N = 2,4,5,6,7,8$) LGT in (3+1)D, as in Fig. 8.

and Aydin [17] are also included for comparison, along with the weak-coupling series prediction [21]. It can be seen that the strong-coupling series estimates are virtually tangent to the weak-coupling prediction at $x \simeq 0.8$, which might suggest a possible second-order transition at that point.

The derivative of the vacuum energy is graphed in Fig. 11. The strong-coupling and weak-coupling extrapola-
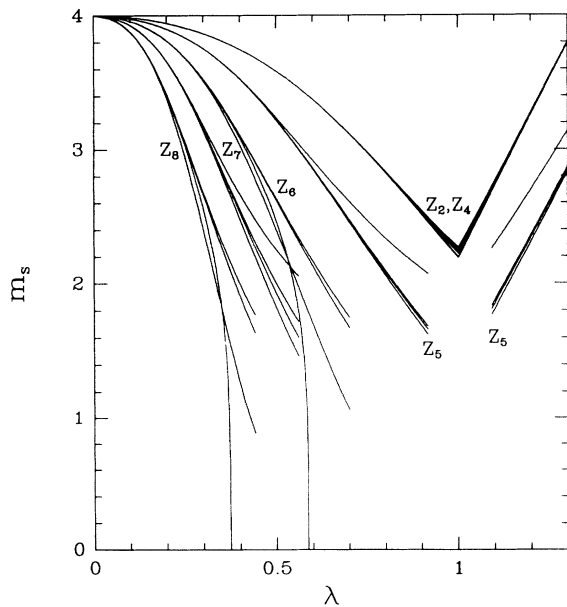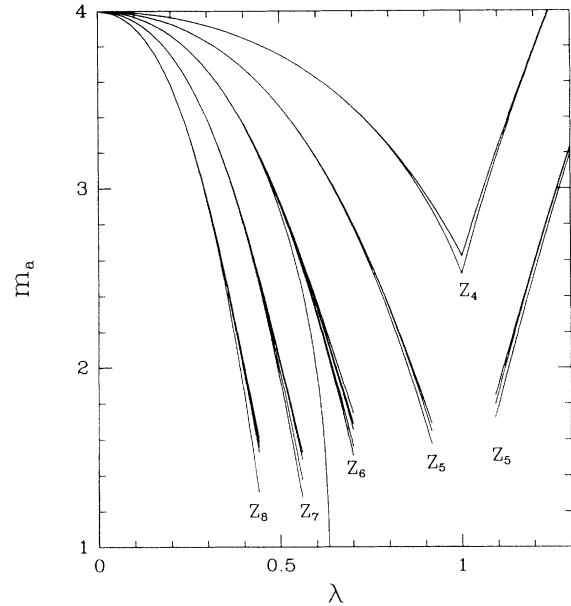

FIG. 8. Graph of the symmetric mass gap m_s against λ (cut off at the critical points deduced from the specific heat series) for the Z_N ($N = 2,4,5,6,7,8$) LGT in (3+1)D. Several different approximants are shown for each model.
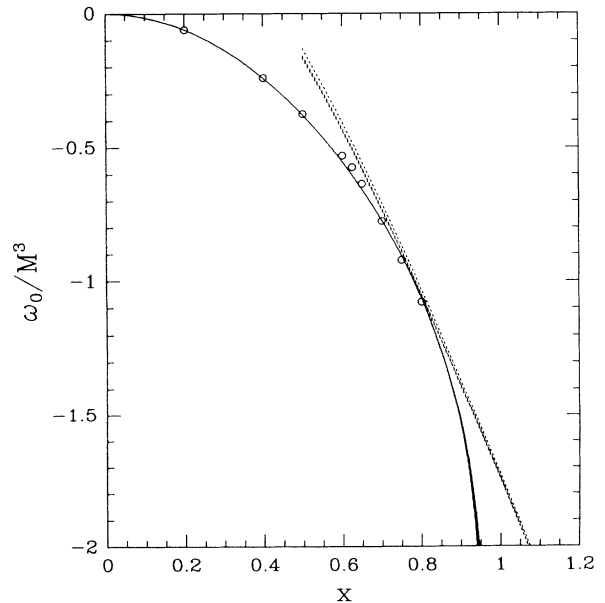

FIG. 10. Graph of the ground-state energy per site ω_0/M^3 against x for the U(1) LGT in (3+1)D. Also shown are the Monte Carlo results [17], as well as Padé extrapolations for the weak-coupling series [21] (dashed lines).
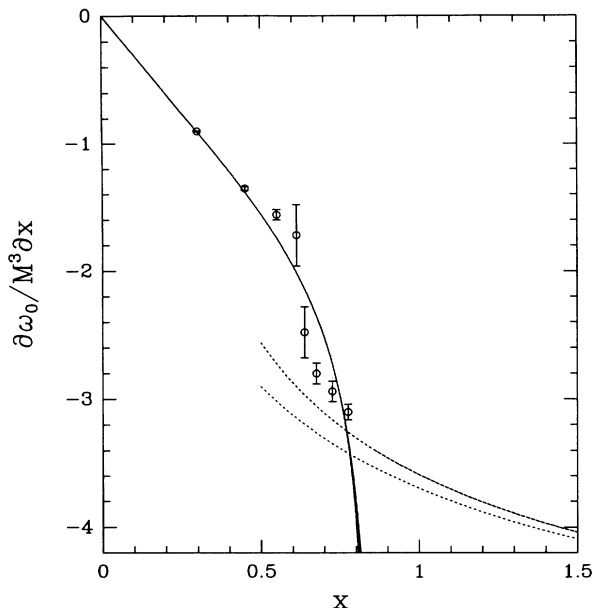
FIG. 11. Graph of the derivative of the ground-state energy per site $\partial\omega_0/M^3\partial x$ against x for the U(1) LGT in (3+1)D. Also shown are the Monte Carlo results [17], as well as Padé extrapolations for the weak-coupling series [21] (dashed lines).

tions cross at $x \simeq 0.81$, and if the transition occurred at this point we would assume it to be second order. In fact, however, the evidence from the Monte Carlo data [17] is that the phase transition occurs somewhat earlier, at $x_c = 0.675 \pm 0.025$.

The strong-coupling series for the specific heat diverges much like that for the Z_6 or Z_8 model. A Dlog Padé
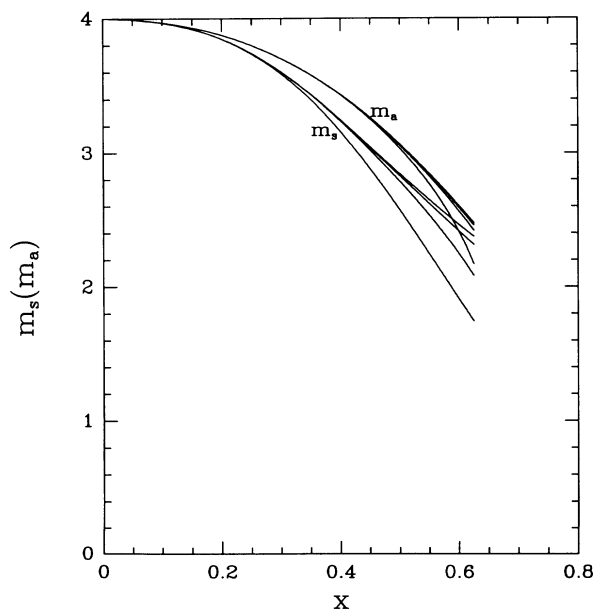

FIG. 12. Graph of the symmetric mass gap m_s and the axial-vector mass gap m_A against x for the U(1) LGT in (3+1)D (cut off at the critical point deduced from the Monte Carlo analysis [17]).

analysis (Table III) indicates a singularity at $x_c^2 = 0.63(8)$ or $x_c = 0.79(5)$, with an index $\alpha = 0.9(3)$, similar to that for the Z_N models.

The specific heat series thus displays evidence of a singularity very close to $x = 0.8$, which lies distinctly *beyond* the true critical point $x_c = 0.675(25)$ obtained from the Monte Carlo data. This indicates that $x = 0.8$ is only a pseudocritical point, and that the transition is indeed first order. This situation is indicated most clearly by the comparison between the series approximants and Monte Carlo estimates in Fig. 11.

For the mass gaps m_s and m_A (Fig. 12), the behavior is qualitatively similar to that for the Z_6 and Z_8 models. A Dlog Padé analysis shows no sign of a stable pole at positive x, and does not help in fixing the phase transition. This may simply be due to the shortness of the series, but it would also seem to indicate that either the mass gap remains finite at the transition (first-order case), or else the index ν is very small (second-order case). Unfortunately there are no Monte Carlo data to compare with for the mass gaps.

IV. SUMMARY AND CONCLUSIONS

Using linked-cluster expansion techniques, new series have been generated for the vacuum energy (and hence the "specific heat") and scalar and axial-vector mass gaps in Abelian lattice gauge theories with Z_N and U(1) symmetry. For Z_N, $N \leq 4$, a first-order transition at the self-dual point was very clearly evident, and estimates of the discontinuities in the latent heat and mass gap were presented. More interesting was the question of the order of the transition for $N \geq 5$ and for the U(1) case.

For the latter cases, series analysis gives clear evidence of a singularity in the specific heat, with an index $\alpha \simeq 0.9$, rather close to the value $\alpha = 1$ which would correspond to a first-order transition. This fact already is going to make it very hard to disentangle whether the transition is first or second order. The mass gap series, on the other hand, show no evidence of a singularity at physical couplings: This may be because the series are too short, or the index ν is small (i.e., the singularity is weak), or else there *is* no singularity.

This situation is the reverse of that for the familiar lattice spin models. There, the index ν is large and the singularity in the mass gap series is strong, while α is small and the singularity in the specific heat series is weak. Normally, if the system undergoes a first-order transition, then one expects the series to display a singularity at a "pseudocritical point" somewhere beyond the true critical point: This can only be detected by a finite-lattice or Monte Carlo calculation, which is not available for the Z_N models.

For the U(1) model, a Monte Carlo simulation is available [17], and it appears that the singularity in the specific heat series does indeed lie beyond the true critical point seen in the Monte Carlo calculation. Taken together with the absence of any sign of a singularity at physical couplings in the mass gap series, this indicates a weak first-order transition, as seen in the Euclidean calculations.

The behavior of the Z_N and U(1) models is qualita-

tively very similar, as one would expect, and it would be interesting to see a Monte Carlo calculation for the Z_5 model, say, to check whether the transition is really first order in this case also.

ACKNOWLEDGMENT

[1] M. Creutz, L. Jacobs, and C. Rebbi, Phys. Rev. Lett. **42**, 1390 (1979); Phys. Rev. D **20**, 1915 (1979).

[2] J.M. Drouffe, Nucl. Phys. **B170**, 91 (1980); M. Falcioni, E. Marinari, M.L. Paciello, G. Parisi, and B. Taglienti, Phys. Lett. **105B**, 51 (1981).

[3] S. Elitzur, R.B. Pearson, and J. Shigemitsu, Phys. Rev. D **19**, 3698 (1979); D. Horn, M. Weinstein, and S. Yankielowicz, *ibid.* **19**, 3715 (1979); A. Ukawa, P. Windey, and A.H. Guth, *ibid.* **21**, 1013 (1980).

[4] B. Bunk, B. Lautrup, and K.J.M. Moriarty, Nucl. Phys. **B251**, 487 (1985).

[5] J.B. Kogut, R.B. Pearson, J. Shigemitsu, and D.K. Sinclair, Phys. Rev. D **22**, 2447 (1980).

[6] J.B. Kogut, D.K. Sinclair, R.B. Pearson, J.L. Richardson, and J. Shigemitsu, Phys. Rev. D **23**, 2945 (1981).

[7] A.C. Irving and C.J. Hamer, Nucl. Phys. **B240**, 362 (1984).

[8] B. Lautrup and M. Nauenberg, Phys. Lett. **95B**, 63 (1980); G. Bhanot, Phys. Rev. D **24**, 461 (1981); T.A. DeGrand and D. Toussaint, *ibid.* **24**, 466 (1981); K.J.M. Moriarty, *ibid.* **25**, 2185 (1982); D.G. Caldi, Nucl. Phys. **B220**, 48 (1983).

[9] T. Jersak, T. Neuhaus, and P.M. Zerwas, Phys. Lett. **133B**, 103 (1983); Nucl. Phys. **B251**, 299 (1985).

[10] R. Gupta, M.A. Novotny, and R. Cordery, Phys. Lett. B **172**, 86 (1986); V. Grösch, K. Jansen, T. Jersak, C.B. Lang, T. Neuhaus, and C. Rebbi, Phys. Lett. **162B**, 171

(1985); A.N. Burkitt, Nucl. Phys. **B270**, 575 (1986); C.B. Lang, *ibid.* **B280**, 255 (1987); V. Azcoiti, G. DiCarlo, and A.F. Grillo, Phys. Lett. B **238**, 355 (1990).

[11] A. Hasenfratz, Phys. Lett. B **201**, 492 (1988).

[12] L.A. Fernandez, A. Munoz Sudupe, R. Petronzio, and A. Tarancon, Phys. Lett. B **267**, 100 (1991).

[13] V. Azcoiti, G. DiCarlo, and A.F. Grillo, Phys. Lett. B **268**, 101 (1991).

[14] J. Kogut, D.K. Sinclair, and L. Susskind, Nucl. Phys. **B114**, 199 (1976).

[15] D.W. Heys and D.R. Stump, Phys. Rev. D **28**, 2067 (1983); **30**, 1315 (1984); S.A. Chin, J.W. Negele, and S.E. Koonin, Ann. Phys. (N.Y.) **157**, 140 (1984); S.E. Koonin, E.A. Umland, and M.R. Zirnbauer, Phys. Rev. D **33**, 1795 (1986).

[16] A.C. Irving and C.J. Hamer, Nucl. Phys. **B235**, 358 (1984).

[17] C.J. Hamer and M. Aydin, Phys. Rev. D **43**, 4080 (1991).

[18] H.X. He, C.J. Hamer, and J. Oitmaa, J. Phys. A **23**, 1775 (1990).

[19] A.J. Guttmann, in *Phase Transitions and Critical Phenomena*, edited by C. Domb and J.L. Lebowitz (Academic, New York, 1974), Vol. 13.

[20] C.J. Hamer and J. Court, Phys. Rev. D **42**, 2835 (1990).

[21] C.J. Hamer and W.H. Zheng, Phys. Rev. D **48**, 4435 (1993).